Comparison of Deconvolution Software

A User Point of View – Part 2

Deconvolution is an image processing technique that restores the effective object representation [3] [4], allowing to improve images analysis steps such as segmentation [1] or colocalization study [2]. We performed several deconvolution tests on different kinds of datasets. The methodology has been reported in Part 1. Evaluation criteria and results are reported here.

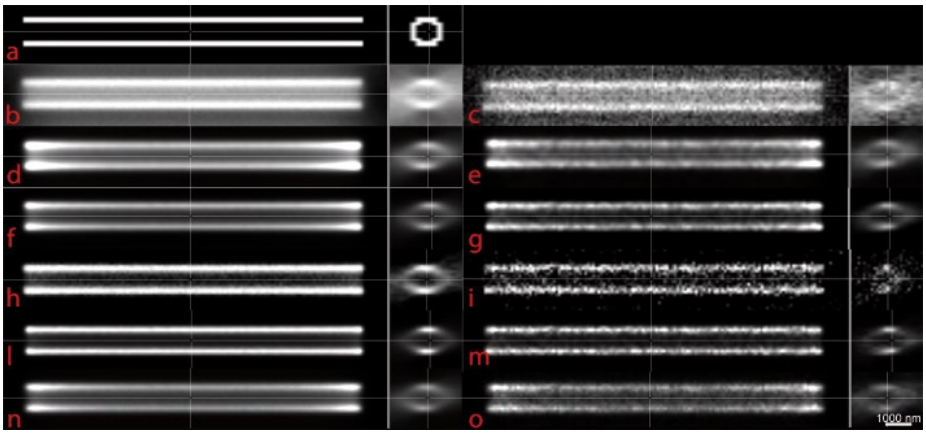

Fig. 1: a) synthetic image (hollow bars) Left column: volume corrupted by Gaussian noise (σ=15) and Poisson noise (SNR = 30) b) and deconvolution results, 40 iterations, HuygensPro (d), AutoDeblur (f), Iterative Deconvolve 3D (h), Parallel Iterative Deconvolution (l), DeconvolutionLab (n). Right column: volume corrupted by Gaussian noise (σ=15) and Poisson noise (SNR = 15) (c) and deconvolution results, 40 iterations, HuygensPro (e), AutoDeblur (g), Iterative Deconvolve 3D (i), Parallel Iterative Deconvolution (m), DeconvolutionLab (o).

Materials and Methods

Evaluation Parameters

The aim of this work is to compare the performance of different deconvolution tools, quantitatively and qualitatively. Therefore we defined a series of evaluation parameters which allows this comparison.

The synthetic dataset is the only one for which we have a ground-truth. As an index of deconvolution efficacy, namely a quantitative indicator of deblurring and noise reduction, we computed the normalized Root Mean Square Error (RMSE) between the deconvolved synthetic volumes and the original one, and between the convolved and noise-corrupted volumes and the original one. We normalized the datasets such as to minimize the RMSE between each couple of images, an important step due to the different dynamic ranges of the deconvolved image between different software results.

Beads images were evaluated by Full Width at Half Maximum (FWHM) on axial and radial intensity profiles passing through the center of the object (fig. 3). This was intended to quantify the resolution improvement indicated by a FWHM closer to the real bead diameter after processing, as expected. Moreover we evaluated the relative contrast between the border and the center of the bead, which is a direct measurement of contrast enhancement. We specifically computed a relative contrast on intensity profiles extracted from the images by normalizing the absolute contrast with respect to the maximum intensity value of the profiles.

Biological images were evaluated by computing the relative contrast on intensity profiles extracted from the FITC channel to quantify contrast enhancement. We evaluated the contrast between separate microtubules (fig. 5). Moreover, for a qualitative evaluation of deconvolution benefits on the biological images, six people (five experts and one naïve user) were asked to judge the results in terms of well defined parameters: sharpness and objects discrimination. *C. elegans* images were also evaluated for the number of protein aggregates labelled with CY3 and detection done automatically or by eye were compared. The automatic spots detection technique was a combination of Gaussian filtering and local maxima detection, without threshold (fig.4).

Finally, to evaluate software performance, we considered the elapsed computation time and peak memory consumption during deconvolution.

Results and Discussion

On the basis of the protocol described in part 1, we performed various deconvolutions on three test datasets, with the aim of comparing the performance of the different tools, quantitatively and qualitatively and also in terms of usability, time and memory usage. Even if it is certainly not possible to draw an absolute ranking of the various packages, we will still highlight their advantages and weak points by the statement of the performed tests. All the evaluation parameters values and results are reported in Table 1.

Quality of the Restoration, Quantitative Considerations

Image deconvolution yields a deblurring of the volume, an indirect noise reduction, a resolution improvement and a contrast enhancement. To quantify and compare these benefits, we computed some quantitative parameters specific to each dataset.

For the synthetic images, for which we have a ground-truth, the normalized Root Mean Squared Error (RMSE) is an indicator of deblurring and noise reduction after deconvolution. As we expected, the reduction of the RMSE respect to the un-deconvolved stack was generally significant, and higher in case of less noise-corrupted images. However comparing the RMSEs, we could notice that AutoDeblur, HuygensPro and DeconvolutionLab showed a superior robustness to noise compared to Parallel Iterative Deconvolution and Iterative Deconvolve 3D. We compared the RMSEs of the synthetic image corrupted by Poisson noise with SNR equal to 30 and equal to 15. We observed that the increase of the RMSEs with the

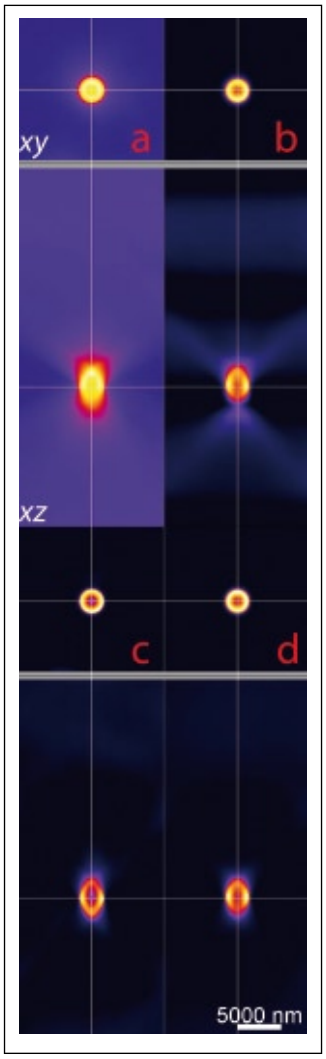

Fig. 2: InSpeck green fluorescent bead, diameter 2.5 µm. Axial and transversal sections. Original image (a) and deconvolution results, 40 iterations: HuygensPro (b), AutoDeblur (c), DeconvolutionLab (d).

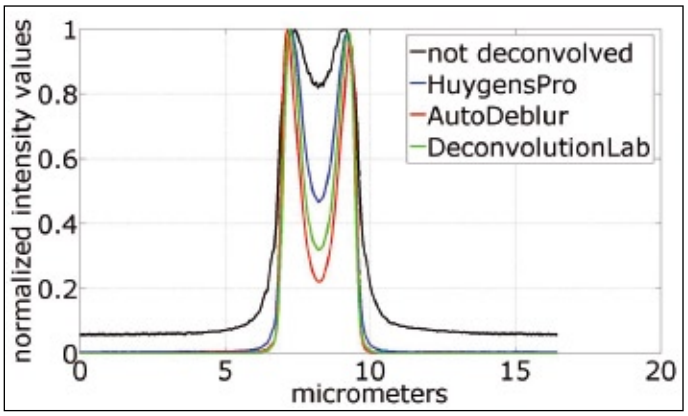

Fig. 3: Radial intensity profiles extracted from original and deconvolved images of an InSpeck green fluorescent bead, diameter 2.5 µm.

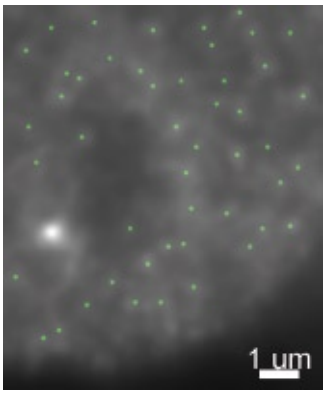

Fig. 4: Detail from the result of deconvolution (HuygensPro, 40 iterations) of *C. elegans* image, CY3 channel. The green spots illustrate the result of the automatic detection of the protein aggregates. Number of spots recognized by eyes: 64. Results of automatic detection: not-deconvolved image 90, HuygensPro result 61, AutoDeblur result 84, DeconvolutionLab result 65.

SNR decrease was much more significant for Parallel Iterative Deconvolution and Iterative Deconvolve 3D. Therefore these two tools appear less robust to noise.

Concerning the bead acquisitions, we report the Full Width at Half Maximums (FWHMs) evaluated on intensity profiles extracted from the images before and after deconvolution. We always observed a reduction of the FWHMs in the results: after deconvolution the bead dimensions were closer to the original ones. This result shows how deconvolution improves resolution. The reduction of bead diameter in the deconvolved image was particularly consistent for the HuygensPro and the DeconvolutionLab results, in the axial direction. To quantify the contrast enhancement, we computed the local relative contrast between the border and the center of the bead. In all the deconvolution results we pointed out contrast amelioration. This amelioration was particularly significant in AutoDeblur results.

From the *C. elegans* images, FITC channel, we evaluated the contrast variation before and after deconvolution between adjacent microtubules (Figure 5). The contrast enhancement was particularly significant in AutoDeblur results.

Quality of the Restoration, Qualitative Considerations

To evaluate the deconvolution results, we always started from a visual inspection of the data.

Figure 1 depicts de-blurring and de-noise effects of deconvolution. We can observe that Parallel Iterative Deconvolution and Iterative Deconvolve 3D give less good results compared to the other tools in case of highly noisy images.

For a qualitative evaluation of the biological volumes restoration, six persons visually judged the deconvolution results. It emerged that the pushed contrast enhancement obtained with AutoDeblur can generate visually less realistic images, with more probable appearance of false structures. Strip-like artefacts have been observed on HuygensPro results (see also fig. 2). The outcomes from AutoDeblur and HuygensPro were nevertheless considered of high level and qualitatively equivalent. The results from DeconvolutionLab were generally judged fuzzier.

Finally we compared the results of automatic and visual detection of spots on the *C. elegans* image, CY3 channel. On the non-deconvolved image the result of the automatic detection was not reliable, as too many local maxima were detected. The numbers of spots detected on HuygensPro and DeconvolutionLab results were similar to the counting by a user (fig. 4).

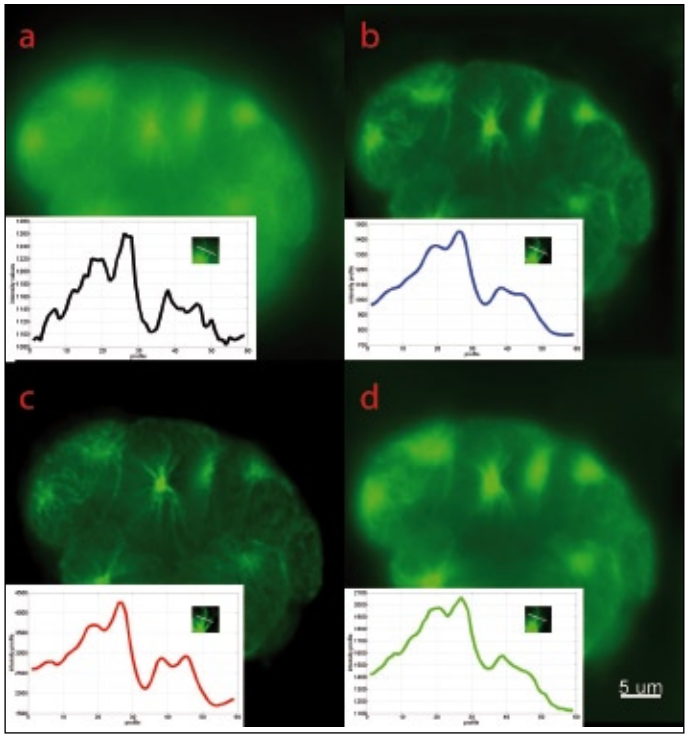

Fig. 5: *C. elegans* embryo, FITC channel. Widefield image, Olympus Cell R, 100X 1.4NA oil objective. Voxel size 64.5 X 64.5 X 200 nm; dimensions 673 X 714 X 111 pixels, 101 MB, 16 bit dynamic range. Transversal sections from the acquired image (a) and from deconvolution results with HuygensPro (b), AutoDeblur (c) and DeconvolutionLab (d), 40 iterations. For each image a particular is reported, together with the same intensity profiles evaluated throughout separate microtubules (note that for the intensity profiles absolute intensities are reported).

Time and Memory Performance

A final important consideration to be done concerns the performance of the tools in terms of runtime and memory consumption, as the deconvolution computational effort is in general particularly heavy. Parallel Iterative Deconvolution and Iterative Deconvolve 3D open-source plugins are inferior in this sense. This is a considerable disadvantage, as the deconvolution can easily fail because of heap memory exception, even for images of common size. On our 10 GB machine we were not able to deconvolve the bead image, 32 MB, and the *C. elegans* image, 101 MB per channel, with these two plugins.

As all the tests were performed on the same machine and in the same conditions, the processing time and the memory consumption of the different tools can be compared, numbers of iterations being equal.

Conclusions

The results of our tests are comparable as we followed a well defined working guideline (Part 1), and the same adequate effort was put into the optimization of deconvolution parameters for all the algorithms.

All the tools that we considered showed good level performance in terms of results quality. With Parallel Iterative Deconvolution and Iterative Deconvolve 3D we were not able to perform all the tests because of out-of-memory exceptions. AutoDeblur showed a particularly high increment of contrast and produced much sharper results. This can facilitate the segmentation but makes the appearance of false structures more probable. HuygensPro produced results that appear more realistic to the expert eye, even if background artefacts were observed in the z direction. DeconvolutionLab showed a particularly good restoration of spatial resolution, but the results were generally considered fuzzier. DeconvolutionLab and HuygensPro showed better performances in terms of time and memory consumption.

Both HuygensPro and AutoDeblur offer different possibilities for image pre-processing, such as background subtraction and spherical aberration corrections, which can certainly further improve the quality of the results but that were not applied in our tests to allow the comparison of the results. Moreover they are particularly user-friendly, especially concerning the setting of the deconvolution parameters. Parallel Iterative Deconvolution and Iterative Deconvolve 3D are addressed to the more expert user as the parameter setting is less immediate. They do not implement pre-processing steps and are open-source software.

Dataset	Parameter	Acquisition	Huygens	AutoDeblur	Dec.Lab	P.I.D.	I.D.3D
RMSE							
synthetic, SNR 30		5070	3010	2850	2880	2790	**2620**
synthetic, SNR 15		6200	3030	**2930**	2940	4420	3370
FWHM (in nm)							
bead	radial	2867	2709	2709	**2664**	–	–
bead	axial	4760	**4000**	4640	4160	–	–
Relative contrast (in %)							
bead		18 %	53 %	**78 %**	68 %	–	–
C. elegans, FITC		15 %	33 %	**50 %**	28 %	–	–
Qualitative evaluation (scale 1 to 5)							
C. elegans	sharpness	n. c.	3.2	**4.2**	2.0	–	–
C. elegans	discrimination	n. c.	3.6	**4.3**	2.2	–	–
Computation time (in s)							
synthetic, SNR 30		n. c.	66	143	**33**	992	1470
bead		n. c.	123	275	**66**	–	–
C. elegans, one channel		n. c.	352	720	**217**	–	–
Memory consumption peak (in MB)							
synthetic		n. c.	**342**	967	434	8821	2054
bead		n. c.	**602**	2439	734	–	–
C. elegans, one channel		n. c.	**1633**	4811	1674	–	–
Deployment							
	Installation/Usage	n.c.	Intuitive	Intuitive	More expert	More expert	More expert
	License	n.c.	Commercial	Commercial	**Open-source**	**Open-source**	**Open-source**
	Platform	n.c	**All**	Win	**All**	**All**	**All**

Tab. 1: The values for the different evaluation parameters with regard to the different datasets are reported. In the 'Acquisition' column the parameters values for the not-deconvolved images or for the simulated acquisition are reported. In the last five columns the parameters values for the deconvolution results with different software (HuygensPro, AutoDeblur, Deconvolution Lab (Dec.Lab), Parallel Iterative Deconvolution (P.I.D.) and Iterative Deconvolve 3D (I.D.3D)) are reported. RMSE: normalized Root Mean Squared Errors between the synthetic image of six parallel hollow bars and the results of deconvolution with the different software. In the 'acquisition' column the RMSEs between the syntethic image and the same image blurred and corrupted by Gaussian and Poisson noise are reported. Radial and axial FWHM: in reference to the bead image, Full Widths Half Maximum evaluated on radial and axial profiles passing through the center of the object. Relative contrast: between the border and the center of the sphere for bead images and between separate microtubules for *C. elegans* images, FITC channel. Qualitative evaluation, scale from 1 (really bad) to 5 (really good); sharpness: capacity of well define objects shape by eyes; discrimination: capacity of distinguish close objects as separate. Runtime and memory consumption peaks. The squares with a dash indicate that it was not possible to complete the deconvolution because of out-of-memory exceptions. 'n.c.' means not computable. We indicated in bold types our favourite choice between software, for the different parameters and datasets.

Acknowledgements

We thank our colleagues José Artacho, Thierry Laroche, J.-C. Floyd Sarria, Jane Kraehenbuehl and Virginie Früh (BIOp group) for their contribution and suggestions. We thank Debora Keller for *C. elegans* samples. We thank SVI and MediaCybernetics for their kind availability and for the demos of the software.

References:

For references, see Part 1.

Authors:
Alessandra Griffa, Nathalie Garin; BioImaging and Optics platform (BIOp), Ecole Polytechnique Fédérale de Lausanne (EPFL)
Daniel Sage; Biomedical Imaging Group (BIG), Ecole Polytechnique Fédérale de Lausanne (EPFL)

Contact:
Nathalie Garin
Leica Microsystems
Heerbrugg, Switzerland
nathalie.garin@leica-microsystems.com